TiO2 Nanoparticles Incorporated Peptide Appended Perylene Bisimide Based Nanohybrid System: Enhancement of Photo-Switching Behavior

Article *in* The Journal of Physical Chemistry C · February 2017

DOI: 10.1021/acs.jpcc.7b00874

CITATIONS
11

READS
264

7 authors, including:

Kingshuk Basu
Hebrew University of Jerusalem
21 PUBLICATIONS **445** CITATIONS

SEE PROFILE

Kousik Gayen
Indian Association for the Cultivation of Science
11 PUBLICATIONS **212** CITATIONS

SEE PROFILE

Arindam Banerjee
Indian Association for the Cultivation of Science
166 PUBLICATIONS **7,047** CITATIONS

SEE PROFILE

THE JOURNAL OF PHYSICAL CHEMISTRY C

Article

pubs.acs.org/JPCC

TiO_2 Nanoparticles Incorporated Peptide Appended Perylene Bisimide-Based Nanohybrid System: Enhancement of Photo-Switching Behavior

Subhasish Roy,[†,§,∥] Kingshuk Basu,[†,∥] Kousik Gayen,[†] Shrabani Panigrahi,[‡] Sulakshana Mondal,[‡] Durga Basak,[‡] and Arindam Banerjee*[,†]

[†]Department of Biological Chemistry, Indian Association for the Cultivation of Science, Jadavpur, Kolkata 700032, India

[‡]Department of Solid State Physics, Indian Association for the Cultivation of Science, Jadavpur, Kolkata 700032, India

Supporting Information

ABSTRACT: A peptide appended perylene bisimide (PBI)-based new hydrogel has been discovered in phosphate buffer medium having the pH ranging from 7.00 to 9.00. This peptide appended PBI-derivative shows interesting photoswitching property in the aggregated state. This gel is thoroughly characterized by UV−visible absorption and fluorescence spectroscopy, field emission scanning electron microscopy (FE-SEM), high resolution transmission electron microscopy (HR-TEM), X-ray diffraction (XRD), and rheological studies. TiO_2 nanoparticles are also prepared by using a protein amino acid, glutamic acid, in water medium. The as-synthesized TiO_2 nanoparticles exhibit usual photoswitching behavior. An organic−inorganic hybrid nanomaterial is prepared by incorporating the as-synthesized TiO_2 nanoparticles into the fibrillar gel network of the native gel. This TiO_2−PBI-based hybrid soft material shows a characteristic of nanofiber and nanoparticle combination in their nanoscale coassembled state as it is evident from the respective TEM images of the hybrid material. Interestingly, this nanohybrid shows improved photoswitching properties (photocurrent gain) compared to that of its individual constituents (TiO_2 nanoparticles and PBI-based xerogel). The increase in photoswitching property holds a future promise for making a new organic−inorganic hybrid material for the optoelectronic device application with a high photocurrent conversion efficiency.

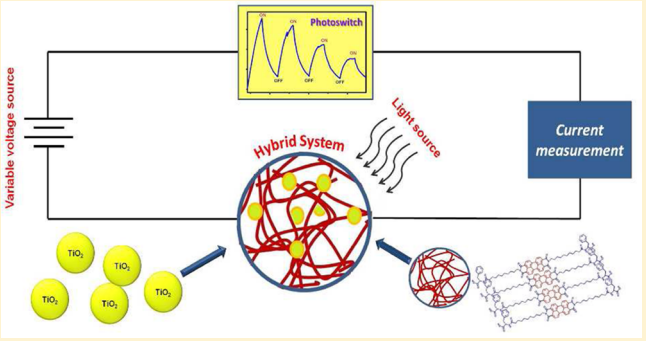

1. INTRODUCTION

Design of π-conjugated new fluorescent gel based soft-materials is an attractive area of current research.[1−5] Though there are several reports on perylene dye based fluorescent organo-gelators,[6−10] perylene bisimide (PBI) appended peptide or amino acid based hydrogels are not well explored[10−20] because the very high hydrophobic flat π-surface of perylene core restricts its processability in aqueous medium.[11,21,22] Making PBI-based electronic devices[23,24] and regulating the photo-switching property of these materials is really challenging.[12,13] There are several reports on photoresponsive/photoswitching gels in the literature from different groups.[25−27] All previously mentioned gels have shown phase transition upon irradiation with particular light source and most of the gelator molecules contain either azobenzene,[26] fumaric amide, and/or dithienyl-cyclopentene[25] moiety. None of these materials have shown the property of photocurrent generation when they were illuminated by a light source.[25−27] In today's scenario the development of alternative energy sources has drawn considerable attention across the world due to the crisis of conventional energy sources. If one can make current from light, then it is one of the cheapest way to make electrical energy from easily available sources. So, to design and develop photocurrent generating system based on organic−organic and/or organic−inorganic hybrid materials is a stepping stone toward the design of such device. There are different techniques to develop photocurrent generating hybrid systems, and self-assembly is one of them involving a donor−acceptor system. Kamat and co-workers have made tremendous efforts in developing semiconducting nanocrystals for application in solar cells, termed solar paint.[28] Park and co-workers have developed highly photoactive, low band gap TiO_2 wrapped by graphene for photocurrent generation.[29] Zhou and co-workers have demonstrated polymeric brush assisted loading of high density CdS/CdSe quantum dots onto TiO_2 nanotubes for photo-electric performances.[30] Wang and co-workers have reported a hybrid TiO_2−Ag nanocluster (NC) photoelectrode showing unique wavelength-switchable photocurrent property.[31] Titanium dioxide (TiO_2) is the most demanding metal oxide used for the development of photoactive material for solar energy conversation in photovoltaic devices as it shows efficient

Received: January 27, 2017
Published: February 8, 2017

DOI: 10.1021/acs.jpcc.7b00874
J. Phys. Chem. C 2017, 121, 5428−5435

photoactivity, higher photocorrosion stability and low cost-effective material.[32−34] However, the low conductivity of TiO_2 is the main obstacle for the possibility to develop an advanced optoelectronic material.[35] TiO_2 nanoparticles-based organic hybrids can be used to enhance the conductivity for the development of future optoelectronic materials. TiO_2 nanocrystals behave as an efficient photocatalyst that have also been reported by several research groups.[36,37] Nanostructured thin films of assembled porphyrin clusters on a TiO_2 electrode under the influence of a dc field has also been applied for light energy conversion.[38] A light sensitive phototransistor based on the composite of poly(3-hexylthiophene) and TiO_2 nanoparticles has also been demonstrated.[39] Photocurrent generation during the photo-oxidation of 4-nonylphenol and 4-nonylphenol polyethoxylate on TiO_2/OTE electrodes have been reported earlier in the literature.[40] In a recent article, Wang and co-workers have reported hydrogen evolution from the PBI dye sensitized Pt/TiO_2 catalyst.[41] However, there is no report on oligomethylene chain containing peptide appended PBI hydrogel that can be applied for generating increased photocurrent upon the inclusion of TiO_2 nanoparticles in a hybrid system. So, it will be interesting to develop a new organic−inorganic hybrid material containing PBI peptide conjugated TiO_2 nanoparticles containing hybrid for enhanced photoswitching behavior.

To address this issue, a peptide appended PBI-based bola-amphiphilic molecule **PBI-P1** has been designed and synthesized. The molecule is designed in such a way that it contains a centrally located PBI unit, a peptide linkage (amide, CONH group at 11-aminoundecanoic acid and phenylalanine junction), and long oligomethylene spacer, so that it can be self-assembled through $\pi-\pi$ interactions by the large aromatic core and terminal phenylalanine moieties, hydrogen bonding interaction through the amide group and van der Waals interaction by oligomethylene chain of 11-aminoundecanoic acid spacer (as illustrated by different colored regions in Figure 1a). In this bola-amphiphilic system, two terminal positions are occupied by polar carboxylic acid groups to increase its solubility in aqueous medium. In the course of our investigation on the self-assembly of these **PBI-P1** molecules, it is found that it forms hydrogels at the pH range 7.00−9.00 in 50 mM phosphate buffer. Figure 1b,c shows the images of the vials containing **PBI-P1** hydrogel at pH 7.5 under daylight and UV irradiation, respectively. It is remarkable to note that this PBI-based aggregated species in xerogel state shows good photoswitching properties.[12,13] TiO_2 nanoparticles generally show good photocurrent generation, photoswitching, and semiconducting properties. Hence, it will be interesting to examine the photoswitching and semiconducting property of TiO_2 nanoparticles containing **PBI-P1** hybrid xerogel to address the question whether there is a significant change in photoswitching behavior of the hybrid system compared to that of its individual components, i.e., **PBI-P1** gel and TiO_2 nanoparticles individually. In this study, the hybrid xerogel consisting of TiO_2 nanoparticles and **PBI-P1** xerogel shows improved photoswitching property than that of its individual components, indicating a good promise for the device applications for this nanohybrid material in future.[42]

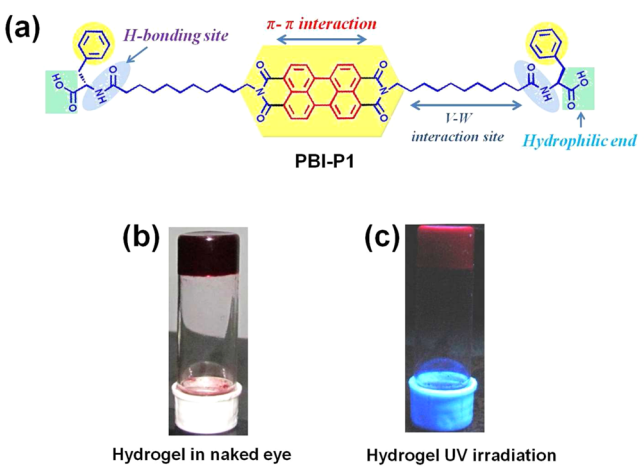

Figure 1. Chemical structure of the hydrogelator (a) and the hydrogels in visible light (b) and under UV light (c) showing its luminescence nature.

2. MATERIALS AND METHODS

2.1. Materials. 11-Aminoundecanoic acid (UNDA) and 3,4,9,10-perylenetetracarboxyldianhydride were purchased from Sigma-Aldrich chemicals. pH paper, sodium dihydrogen phosphate, and disodium hydrogen phosphate were purchased from Merck. L-Phenylalanine (F), imidazole, liquid ammonia, sodium chloride, sodium carbonate, sodium hydroxide, 35% hydrochloric acid, di-*tert*-butyl pyrocarbonate (Boc-anhydride), methanol, DCC (dicyclohexylcarbodiimide), titanium isopropoxide, L-glutamic acid, and 98% formic acid were purchased from SRL. HOBt (1-hydroxybenzotriazole) in the form of monohydrate was purchased from Spectrochem chemicals.

2.2. Synthesis of TiO_2 Nanoparticles. TiO_2 nanoparticles have been synthesized using a reported procedure.[43] 1 g of L-glutamic acid (6.8 mmol) was added with 20 mL of milli-Q water with proper stirring. The pH of the solution was maintained toward neutral by using 1 M sodium hydroxide solution. A titanium isopropoxide [$Ti(OiPr)_4$] solution was prepared by adding 1 mL of $Ti(OiPr)_4$ in 5 mL of isopropyl alcohol (3.4 mmol). This solution was then slowly added into the glutamic acid solution. The pH of the mixed solution was then adjusted to pH 10 by adding an ammonia solution (25%) and stirred for 2 h at room temperature. The resultant solid was collected by repeated centrifugation (10000 rpm, 15 min) and washing with milli-Q water. The material was dried in oven at 383 K for overnight. The as-synthesized TiO_2 nanoparticles have been used for this study.

2.3. Synthesis of [*N*,*N*′-Di(2-(11-aminoundecanamido-L-phenylalanine)-perylene-3,4:9,10-tetracarboxylic acid bisimide]-(PBI-P1). Synthetic procedure and detailed characterizations of the molecule have been discussed in detail in the Supporting Information.

2.4. Preparation of Hydrogel with PBI-P1. To make hydrogel from the gelator (**PBI-P1**) we have used four different types of pHs of phosphate buffer of strength 50 mM. Gelator compound and phosphate buffer solution of desired pH were taken in a well capped glass vial and the vial was then strongly warmed on a hot plate to dissolve then cooled to room temperature to get a dark red hydrogel.

2.5. Preparation of Hybrid Hydrogel with PBI-P1 and TiO_2. To make each set of hybrid gel, 4 mg of TiO_2 nanoparticles were taken in a glass vial. Then it was dispersed in a 1 mL aqueous solution of phosphate buffer of pH 7.5 by repetitive tip sonication. A total of 40 mg of powder of **PBI-P1** was then added to the dispersion, which was then subjected to a number of heating cooling cycles and kept at room temperature

DOI: 10.1021/acs.jpcc.7b00874
J. Phys. Chem. C 2017, 121, 5428−5435

(25−30 °C) for a few hours to get a dark red gel. The amount of TiO_2 nanoparticle was standardized to 4 mg with respect to 40 mg of **PBI-P1** gelator, by trial and error to get a hybrid material with the most convincing photoconductance.

3. RESULTS AND DISCUSSIONS

The peptide appended PBI gelator is found to form hydrogel within the pH range 7.00−9.00 in phosphate buffer. A detailed description for gel formation including minimum gelation concentration (MGC) in different pHs are given in the Supporting Information. Upon irradiation with UV light at 365 nm this gel shows a bright red color, Figure 1.

3.1. UV−vis Spectroscopic Study. UV−vis spectroscopic analysis of the gelator molecule was carried out to examine aggregation behavior of **PBI-P1** in hydrogel. UV−vis spectroscopic studies of **PBI-P1** were performed in both nonaggregating (ethanol) and aggregating (water) solvents at pH 7.5 (Figure 2a). Figure 2a shows that the spectra of **PBI-P1**

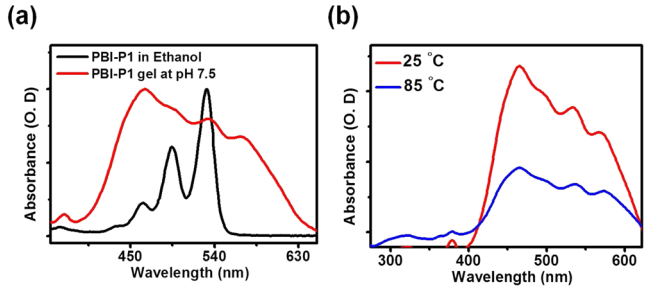

Figure 2. (a) UV−vis spectra of monomeric **PBI-P1** in ethanol and hydrogel of the same compound at pH 7.5, (b) UV−vis absorption profiles at two different temperatures [25 °C (hydrogel) and 85 °C (solution of hydrogel)].

in aggregating gel state is broader than that of nonaggregated monomeric state. The broadening of absorption peaks is observed due to face to face H-type aggregation involving $\pi-\pi$ stacking of PBI units present in the molecule, and this triggers an increased conductance of the aggregates.[44] A difference in absorption pattern was also found in the gel state and sol state of the compound in aqueous medium. In the gel state at 25 °C, absorption peaks at 465, 534, and 569 nm along with a small hump at 496 nm have been observed, whereas at an elevated temperature of 85 °C (where the gel melts) the peaks at 465, 537, and 574 nm along with a small hump at 496 nm have been observed. Thus, temperature dependent UV−vis spectroscopic study (Figures 2b and S3) clearly illustrated that during the process of increasing temperature the absorbance has decreased along with a red shifting from gel state to solution state. The red shifting of two major peaks (534 and 569 nm to 537 and 575 nm, respectively, with a very low intensity, i.e., the band almost disappeared at higher temperature) from gel state to solution state vividly demonstrate that the formation of π-stacked H-aggregate in gel state.[12]

3.2. Fluorescence Spectroscopic Analyses. Fluorescence spectroscopic studies of **PBI-P1** have been performed at two different concentrations in pH 7.5 buffer at 0.004×10^{-6} (M) concentration where gelation does not take place and at 0.308×10^{-6} (M) concentration where gel is formed (Figure 3, excitation and emission spectra shown in Figure 4). The emission peak of dilute solution is at 460 nm, and it has been shifted to 688 nm in the gel state. The red shift of the emission

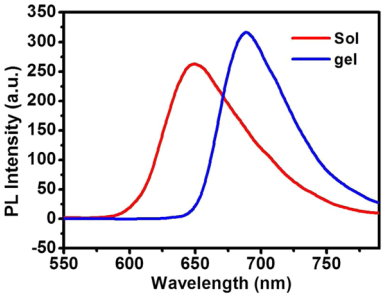

Figure 3. Fluorescence emission profiles of the hydrogelator in solution (sol) and in gel state for excitation at 639 nm.

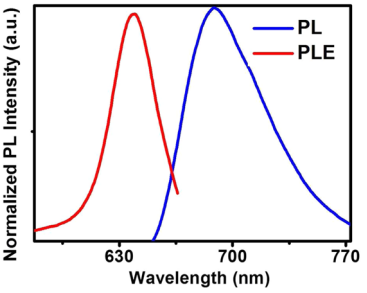

Figure 4. Fluorescence emission (PL; emission peak at 688 nm) and fluorescence excitation (PLE; excitation peak at 639 nm) spectra profiles of the **PBI-P1** hydrogel.

peak in the fluorescence spectra can be due to the formation of an "excimer-like" state of PBI. From UV−vis absorption study we previously found a signature of H-type aggregate which may be due to columnar stacking of the PBI core.[45,46] This excimeric interaction among molecular aggregates also facilitates charge transport along the aggregation axis of the molecules; that is, the electrical conduction of gelators increases.[47]

A pH-dependent fluorescence study has also been performed to understand how the pH of the gelating solvent affects the emission behavior of **PBI-P1** aggregates. At pH 7.00 the hydrogel at its MGC shows fluorescence emission maxima at 682 nm. However, due to the increase in pH from pH 7.00 to 9.00, the fluorescence emission has been changed from 682 to 696 nm (Figure S4). Interestingly, at pH 7.5 and 8.00 hydrogels show fluorescence emission near 688 nm (Figure S4). However, at pH 9.00 the emission band has shifted toward red and may be due to the much more aggregated excited state species generated than lower pH. So, in each pH's hydrogel shows the emission peak for their excimer-like complex and due to increase in pH the excited species shows emission at higher region suggesting the more aggregation behavior of the gelator at higher pH and also the change of interacting species in their self-assembled state.

3.3. TCSPC. Time correlated single photon counting spectroscopic study has also been performed to know the lifetime of the fluorescent hydrogel in excited state. The decay profile of the hydrogel has been shown in Figure S5 of the Supporting Information. The average lifetime of the hydrogel has been estimated to be 0.5 ns at pH 7.5 at its MGC.

3.4. Microscopic Analyses. *3.4.1. Morphology of the Native Hydrogel. 3.4.1.1. Transmission Electron Microscopic Analysis.* The microscopic morphological insight has also been determined from transmission electron microscopy (TEM) study. Figure 5a,b shows the TEM images of **PBI-P1** xerogel. It

DOI: 10.1021/acs.jpcc.7b00874
J. Phys. Chem. C 2017, 121, 5428−5435

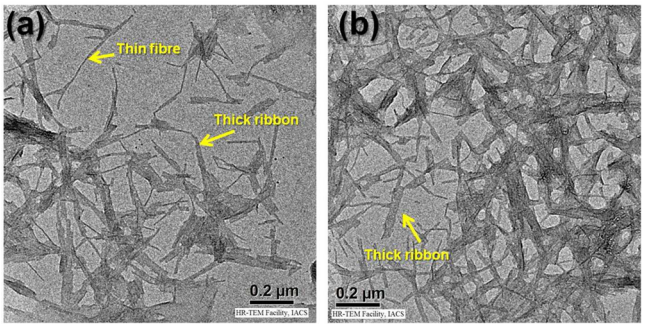

Figure 5. (a and b) TEM images of the **PBI-P1** dried gel.

is evident from these TEM images that in the gel state nanoribbons are formed. Thinner nanofibers are also present with a few nanometer width and several micrometers in length. The dimension of fiber to ribbon varies from 7 to 50 nm. So, it can be envisioned that small fibers has self-assembled to form thick ribbon like morphology. It is clear from the TEM images that fibers obtained from the low concentration are smaller in length and thinner in width than that of the nanofibers obtained from the relatively concentrated solution of gel phase. So it can be concluded that the fibers are becoming thicker as the concentration goes up from solution to gel.

3.4.2. Morphology of TiO_2 Nanoparticles. 3.4.2.1. Transmission Electron Microscopic Analysis. The TEM study of as-prepared TiO_2 nanoparticles has been performed to examine the morphology of the nanoparticles. Figure S6a shows that TiO_2 nanoparticles are spherical in shape and very small in size with an average diameter of 2 nm. SAED pattern of TiO_2 nanoparticles has been shown in Figure S6b representing the (204) plane of the anatase phase.

3.4.3. Morphology of TiO_2 Containing Hybrid PBI-Based Hydrogel. It is interesting to explore the morphology of TiO_2 nanoparticles incorporated hybrid hydrogel of **PBI-P1** gelator. The TEM images in Figure 6 vividly exhibit the presence of two kinds of morphological features namely nanofibers (coming from PBI-based self-assembled system) and spherical nanoparticles (coming from TiO_2 nanoparticles) inside the hybrid gel. An enlarged view of Figure 6a, Figure 6b and Figure 6c suggest TiO_2 nanoparticles are decorated on the gel nanofibers. Energy-dispersive X-ray spectroscopic analysis (Figure S7) shows that the presence of Ti within the hybrid hydrogel based material.

3.5. FT-IR Study. FT-IR spectroscopy of the freeze-dried sample was done to check internal molecular interactions of the gel phase material (Figure S8 of Supporting Information). The peak at 1653 cm^{-1} indicates the presence of weekly hydrogen bonded C═O and broad peak at 3420 cm^{-1} indicates the presence of free N−H of amide. Interestingly peaks at 1692, 1588, and 1400 cm^{-1} range are present in the FT-IR spectra of xerogel, which signifies that both carboxylic acid (−COOH) and carboxylate anion ($-COO^-$) group are coexistant in gel phase, in the other words it can be stated that terminal acid group is present in both protonated and deprotonated form (Figure S8).[48,49]

3.6. X-ray Diffraction Analyses. *3.6.1. X-ray Diffraction Analysis of Native Xerogel.* Wide angle X-ray diffraction pattern of the native xerogel has been shown in Figure 7. Figure

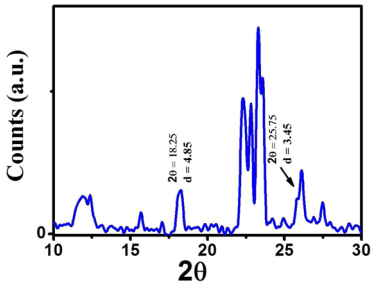

Figure 7. Wide angle X-ray diffraction pattern of the xerogel of **PBI-P1**.

7 clearly shows the existence of a small peak at 2θ = 18.25 corresponding to the d value of 4.8 Å suggesting the presence of hydrogen bonded sheet-like assembly within the xerogel network structure. Another peak at 2θ = 25.75 corresponding to the d value of 3.45 Å may be due to the presence of π-stacked planes.[50] However, small-angle X-ray diffraction analysis (Figure S9) shows the existence of a peak at 2θ = 1.38° corresponding to the d = 64.16 Å representing the existence of self-assembled state with a length more than molecular length (calculated from chem. draw. 3D). Including small-angle X-ray diffraction analysis and wide-angle X-ray diffraction analysis it can be mentioned that the **PBI-P1** molecules are self-assembled to form a network structure using hydrogen bonding as well as $\pi-\pi$ interactions to form a hydrogel.

3.6.2. X-ray Diffraction Analysis of TiO_2 Nanoparticles. X-ray diffraction profile for the calcinated TiO_2 nanoparticles has been shown in Figure S10 showing the presence of peaks at 2θ = 37. 80 (004), 48.17 (200), 54.04 (105), 55.18 (211), 62.91 (204), 69.00 (116), 70.18 (220), 75.19 (215) corresponding to the anatase phase. We have also performed X-ray diffraction study of TiO_2 nanoparticles before calcinations, however, the diffraction pattern is not so prominent in their ligand stabilized

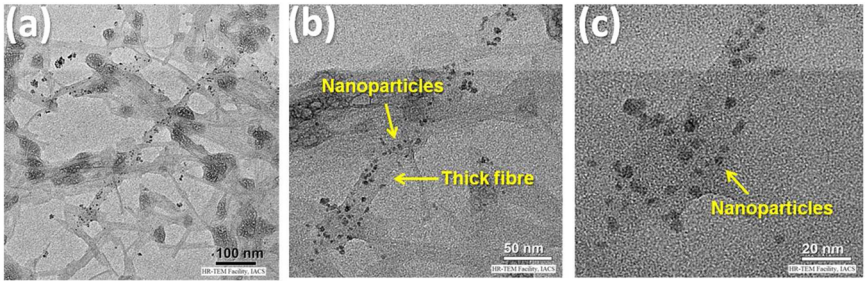

Figure 6. (a) TEM images of TiO_2 nanoparticles containing **PBI-P1** based hybrid dried gel showing the presence of both nanoparticles and nanofibers, and panels b and c are the enlarged view of panel a showing the deposition of nanoparticles on the hydrogel nanofibers.

DOI: 10.1021/acs.jpcc.7b00874
J. Phys. Chem. C 2017, 121, 5428−5435

nanoparticles form (Figure S11). Due to the presence of organic ligand in their surface the crystalline nature has diminished and thus the X-ray diffraction pattern is not sharp and various peaks missing.

3.7. Rheology. Viscoelastic behavior of the native hydrogel as well as the hybrid hydrogel have been performed using rheological experiments to measure the stiffness of the native hydrogel and also to address the question whether mechanical strength of the hybrid hydrogel is changed after the incorporation of TiO_2 nanoparticles into the native gel. Storage modulus (G') and loss modulus (G'') at a constant strain of 0.002 was measured. In Figure 8, G' and G'' have been plotted

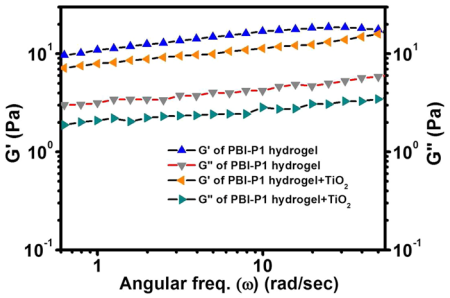

Figure 8. Storage modulus (G') and loss modulus (G'') vs angular frequency profile for the **PBI-P1** supramolecular native hydrogel and 0.4% w/v and TiO_2 containing **PBI-P1** based hybrid hydrogel.

against angular frequency for both native and hybrid hydrogel. In both cases storage and loss modulus are almost parallel to the angular frequency change within the experimental range and G' is greater than G'' within the angular frequency range. It suggests the viscoelastic behavior of both native and hybrid hydrogels. It is apparent from Figure 8 that G' values for the native gel and the hybrid gel containing TiO_2 nanoparticles are within the comparable range. These rheological experiments were repeated for several times, and error bars (calculated by standard deviation method) were mentioned. This figure is shown in the Supporting Information (Figure S12).

3.8. Photoswitching Behavior. For the photoresponse study, a simple conductor device in planar geometry was fabricated by evaporating two Au contacts of area 1 mm separated by a distance of 3 mm on pellets made of **PBI-P1** xerogel, TiO_2 nanoparticles and PBI-TiO_2 hybrid xerogel (the inset in Figure 9). Then, the required light from a xenon lamp

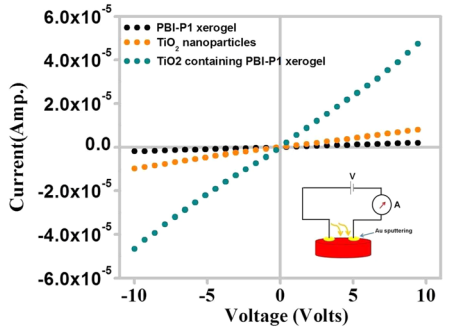

Figure 9. Plots of $I-V$ curves of a simple conductor device made of **PBI-P1** xerogel, TiO_2 nanoparticles, and TiO_2 containing **PBI-P1** based hybrid xerogel in dark condition. Inset: A schematic representation of the layout of the circuit diagram for $I-V$ measurements.

(model no. 66902; Newport Corp. USA) was shined on the conductor area to measure the photoresponse properties of the corresponding pellets. The current between the two contacts were measured using a Keithley source meter (model 2400). Dark current−voltage ($I-V$) plot in both positive and negative bias show almost Ohmic behavior for all the specimens (Figure 9). Interestingly, conductivity has been sharply increased for the hybrid xerogel. The increase in conductance in the hybrid system can be due to the synergistic effect of both semiconducting materials namely **PBI-P1** nanofibers and TiO_2 nanoparticles. Upon irradiation with white light from the Xe source in all cases, effectively the conductivity is increased, but the amount of surge in photocurrent is significantly high for the hybrid system as composed of other two components (Figure 10; enlarged view of photoswitching

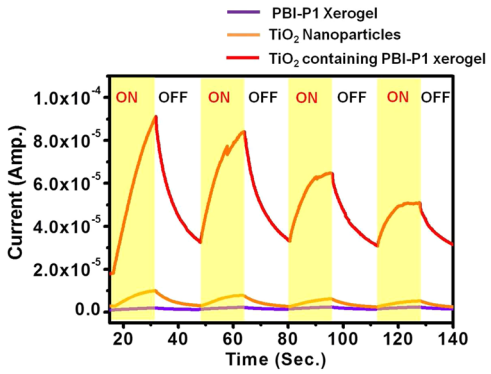

Figure 10. Transient photoresponse by turning on/off white light illumination of a representative conductor device made of **PBI-P1** xerogel, TiO_2 nanoparticles, and TiO_2 containing **PBI-P1** based hybrid xerogel.

pattern of TiO_2 nanoparticles and **PBI-P1** xerogel are shown in Figure S13 of the Supporting Information). For TiO_2 nanoparticles and **PBI-P1** xerogel the increase in current (I_{on}/I_{off}) upon irradiation of white light is 2.67 and 1.95 times, respectively, but for the hybrid xerogel, the increase in current upon irradiation is 4.5 fold, and this is a very interesting observation (Table 1). The amount of photocurrent has also been increased drastically. All results have been checked multiple times and found to be fairly repeatable. PBI containing dyes can absorb a long-range of light from visible spectrum; therefore, these moieties are good antenna of light absorption, after the absorption of photon they form a electron and hole pair. The photoexcited electron of the PBI moiety then goes to the conduction band of TiO_2 nanoparticles due to comparable position of the excited states of PBI moiety and the conduction band of TiO_2 nanoparticles in their respective energy levels and as a result of that a huge photocurrent value is observed for hybrid xerogels containing PBI-based peptide and TiO_2 nanoparticles.[41,51,52] This type of organic−inorganic photo-responsive hybrid system is very important in future device application due to their easy processability and cheap cost. It is worth notable that the ON-state current decreases slowly with number of cycles. However, no current degradation has been noted, when the experiment is repeated after keeping the pellet in vacuum for 3 h (Figure S14 of the Supporting Information). This kind of decay in photocurrent may be due to the presence of a moisture layer or trapped oxygen in the pellet and after keeping at high vacuum such interfering species are vanished. It

DOI: 10.1021/acs.jpcc.7b00874
J. Phys. Chem. C 2017, 121, 5428−5435

Table 1. Dark and Photocurrent Generated by Individual and Hybrid Systems and Their Current Ratio[a]

sample	dark current (Amp)	photo current (Amp)	gain (I_{on}/I_{off})
TiO_2	$(2.56 \pm 0.221) \times 10^{-6}$	$(6.83 \pm 2.369) \times 10^{-5}$	2.67
PBI-P1	$(1.13 \pm 0.170) \times 10^{-6}$	$(2.21 \pm 0.189) \times 10^{-6}$	1.95
PBI-P1 + TiO_2	$(2.02 \pm 0.262) \times 10^{-5}$	$(9.05 \pm 0.072) \times 10^{-5}$	4.48

[a]Measured at 10 V with standard deviation within brackets.

is found that after keeping these samples 1 day in open air, such impurity reappears and the photocurrent decreases again.

3.9. Wavelength response of Photocurrent. From the UV−vis analysis we have already found that the dye molecules have distinct absorption peaks (Figure 2a). So, it is interesting to check whether there is any wavelength dependency on photocurrent generation of these xerogels. In this regard, all conductor devices were exposed to light with different wavelengths and their current response was measured with varying wavelength. Figure S15 of the Supporting Information shows wavelength dependency of hybrid xerogel and their components (i.e., native xerogel and TiO_2 nanoparticles) on photocurrent generation. The native gel does not show any significant change in photocurrent with an alteration of wavelength (Figure S15a of the Supporting Information), whereas the TiO_2 nanoparticles have strong wavelength dependency at 375 and 565 nm (Figure S15b of the Supporting Information). Interestingly, it is found that the hybrid xerogel containing TiO_2 nanoparticles shows a weak wavelength dependency within the range of 300−600 nm; however, it is not so significant like the TiO_2 nanoparticles alone. This happens due to the fact that the hybrid gel contain higher amount of **PBI-P1** than TiO_2 nanoparticles. So, it can be stated that the hybride xerogel shows a significant wavelength dependency on photocurrent compared to the native xerogel due to incorporation of TiO_2 nanoparticles.

4. CONCLUSIONS

The peptide containing perylene bisimide-based molecule (**PBI-P1**) forms hydrogels upon assembly in water within the pH range 7.00−9.00, with a nanofibrous network forming morphology. This gel based soft material not only exhibits a bright red fluorescence but also displays a good photoswitching property. Moreover, upon incorporation of TiO_2 nanoparticles within this **PBI-P1** gel, an excellent, new organic−inorganic nanohybrid system with nanoparticles and nanofibers forms. This hybrid has shown a remarkable enhancement in photoswitching behavior with a photocurrent again compared to that of its individual constituents (TiO_2 nanoparticles/**PBI-P1** hydrogel). This synergistic effect for the photocurrent generation in this new hybrid system holds a future promise for making a thin film of a new organic−inorganic hybrid material for optoelectronic device applications.

■ ASSOCIATED CONTENT

Supporting Information

The Supporting Information is available free of charge on the ACS Publications website at DOI: 10.1021/acs.jpcc.7b00874.

Synthetic details and spectral analysis of gelator molecule **PBI-P1**. Figures and curves for microscopic, spectroscopic, rheological, and photoelectric (photoswitching) studies of the hydrogels (both native and hybrid gel). (PDF)

■ AUTHOR INFORMATION

Corresponding Author

*Tel: +91 33 2473 4971. E-mail: bcab@iacs.res.in.

ORCID

Durga Basak: 0000-0002-0149-1513

Arindam Banerjee: 0000-0002-1309-921X

Present Address

§Department of Materials Engineering, Ben Gurion University of the Negev Beer-Sheva 84105, Israel.

Author Contributions

‖S.R. and K.B. contributed equally.

Notes

The authors declare no competing financial interest.

■ ACKNOWLEDGMENTS

K.B. and K.G. gratefully acknowledge CSIR for funding supports.

■ REFERENCES

(1) Babu, S. S.; Praveen, V. K.; Ajayaghosh, A. Functional π-Gelators and Their Applications. *Chem. Rev.* **2014**, *114*, 1973−2129.

(2) Sugiyasu, K.; Kawano, S.-i; Fujita, N.; Shinkai, S. Self-Sorting Organogels with p-n Heterojunction Points. *Chem. Mater.* **2008**, *20*, 2863−2865.

(3) Gao, C.; Xue, L.; Chen, Y.; Li, X. Supramolecular Organogels Based on Perylenetetracarboxylic Diimide Trimers Linked with Benzenetricarboxylate. *Colloid Polym. Sci.* **2015**, *293*, 35−48.

(4) Kandanelli, R.; Maitra, U. Charge-transfer Interaction Mediated Organogels from Bile Acid Appended Anthracenes: Rheological and Microscopic Studies. *Photochem. Photobiol. Sci.* **2012**, *11*, 1724−1729.

(5) Berdugo, C.; Nalluri, S. K. M.; Javid, N.; Escuder, B.; Miravet, J. F.; Ulijn, R. V. Dynamic Peptide Library for the Discovery of Charge Transfer Hydrogels. *ACS Appl. Mater. Interfaces* **2015**, *7*, 25946−25954.

(6) Würthner, F.; Saha-Möller, C. R.; Fimmel, B.; Ogi, S.; Leowanawat, P.; Schmidt, D. Perylene Bisimide Dye Assemblies as Archetype Functional Supramolecular Materials. *Chem. Rev.* **2016**, *116*, 962−1052.

(7) Wu, H.; Xue, L.; Shi, Y.; Chen, Y.; Li, X. Organogels Based on J- and H-Type Aggregates of Amphiphilic Perylenetetracarboxylic Diimides. *Langmuir* **2011**, *27*, 3074−3082.

(8) Lin, X.; Hirono, M.; Kurata, H.; Seki, T.; Maruya, Y.; Nakayama, K.-i; Yagai, S. A Perylene Bisimide Organogelator for Chlorinated Solvents. *Asian J. Org. Chem.* **2014**, *3*, 128−132.

(9) Lin, X.; Hirono, M.; Seki, T.; Kurata, H.; Karatsu, T.; Kitamura, A.; Kuzuhara, D.; Yamada, H.; Ohba, T.; Saeki, A.; et al. Covalent Modular Approach for Dimension-Controlled Self-Organization of Perylene Bisimide Dyes. *Chem. - Eur. J.* **2013**, *19*, 6561−6565.

(10) Bai, S.; Debnath, S.; Javid, N.; Frederix, P. W. J. M.; Fleming, S.; Pappas, C.; Ulijn, R. V. Differential Self-Assembly and Tunable Emission of Aromatic Peptide Bola-amphiphiles Containing Perylene Bisimide in Polar Solvents Including Water. *Langmuir* **2014**, *30*, 7576−7584.

(11) Görl, D.; Zhang, X.; Würthner, F. Molecular Assemblies of Perylene Bisimide Dyes in Water. *Angew. Chem., Int. Ed.* **2012**, *51*, 6328−6348.

DOI: 10.1021/acs.jpcc.7b00874
J. Phys. Chem. C 2017, 121, 5428−5435

(12) Roy, S.; Maiti, D. K.; Panigrahi, S.; Basak, D.; Banerjee, A. A New Hydrogel from an Amino Acid-Based Perylene Bisimide and Its Semiconducting, Photo-Switching Behaviour. *RSC Adv.* **2012**, *2*, 11053−11060.
(13) Roy, S.; Maiti, D. K.; Panigrahi, S.; Basak, D.; Banerjee, A. A Bolaamphiphilic Amino Acid Appended Photo-Switching Supramolecular Gel and Tuning of Photo-Switching Behaviour. *Phys. Chem. Chem. Phys.* **2014**, *16*, 6041−6049.
(14) Datar, A.; Balakrishnan, K.; Zang, L. One-dimensional Self-assembly of a Water Soluble Perylene Diimide molecule by pH Triggered Hydrogelation. *Chem. Commun.* **2013**, *49*, 6894−6896.
(15) Draper, E. R.; Walsh, J. J.; McDonald, T. O.; Zwijnenburg, M. A.; Cameron, P. J.; Cowan, A. J.; Adams, D. J. Air-stable Photoconductive Films Formed from Perylene Bisimide Gelators. *J. Mater. Chem. C* **2014**, *2*, 5570−5575.
(16) Dwivedi, A. K.; Pandeeswar, M.; Govindaraju, T. Assembly Modulation of PDI Derivative as a Supramolecular Fluorescence Switching Probe for Detection of Cationic Surfactant and Metal Ions in Aqueous Media. *ACS Appl. Mater. Interfaces* **2014**, *6*, 21369−21379.
(17) Sukul, P. K.; Singh, P. K.; Maji, S. K.; Malik, S. Aggregation Induced Chirality in a Self Assembled Perylene Based Hydrogel: Application of the Intracellular pH Measurement. *J. Mater. Chem. B* **2013**, *1*, 153−156.
(18) Sukul, P. K.; Asthana, D.; Mukhopadhyay, P.; Summa, D.; Muccioli, L.; Zannoni, C.; Beljonne, D.; Rowan, A. E.; Malik, S. Assemblies of Perylene Diimide Derivatives with Melamine into Luminescent Hydrogels. *Chem. Commun.* **2011**, *47*, 11858−11860.
(19) Bairi, P.; Roy, B.; Nandi, A. K. Bi-component Hydrogel of Perylene-3,4,9,10-tetracarboxylic Potassium Salt and L-tyrosine. *RSC Adv.* **2012**, *2*, 264−272.
(20) Draper, E. R.; Mykhaylyk, O. O.; Adams, D. J. Aligning Self-assembled Gelators by Drying Under Shear. *Chem. Commun.* **2016**, *52*, 6934−6937.
(21) Tang, T.; Herrmann, A.; Peneva, K.; Müllen, K.; Webber, S. E. Energy Transfer in Molecular Layer-by-Layer Films of Water-Soluble Perylene Diimides. *Langmuir* **2007**, *23*, 4623−4628.
(22) Krieg, E.; Rybtchinski, B. Noncovalent Water-Based Materials: Robust yet Adaptive. *Chem. - Eur. J.* **2011**, *17*, 9016−9026.
(23) Rybak, A.; Pfleger, J.; Jung, J.; Pavlik, M.; Glowacki, I.; Ulanski, J.; Tomovic, Z.; Müllen, K.; Geerts, Y. Charge Carrier Transport in Layers of Discotic Liquid Crystals as Studied by Transient Photocurrents. *Synth. Met.* **2006**, *156*, 302−309.
(24) Chen, S.; Slattum, P.; Wang, C.; Zang, L. Self-Assembly of Perylene Imide Molecules into 1D Nanostructures: Methods, Morphologies, and Applications. *Chem. Rev.* **2015**, *115*, 11967−11998.
(25) Xie, F.; Qin, L.; Liu, M. A Dual Thermal and Photo-switchable Shrinking−swelling Supramolecular Peptide Dendron Gel. *Chem. Commun.* **2016**, *52*, 930−933.
(26) Yamaguchi, H.; Kobayashi, Y.; Kobayashi, R.; Takashima, Y.; Hashidzume, A.; Harada, A. Photoswitchable Gel Assembly Based on Molecular Recognition. *Nat. Commun.* **2012**, *3*, 603.
(27) Tang, Q.; Nie, Y.-T.; Gong, C.-B.; Chow, C.-F.; Peng, J.-D.; Lam, M. H.-W. Photo-Responsive Molecularly Imprinted Hydrogels for the Detection of Melamine in Aqueous Media. *J. Mater. Chem.* **2012**, *22*, 19812−19820.
(28) Christians, J. A.; Herrera, P. A. M.; Kamat, P. V. Transformation of the Excited State and Photovoltaic Efficiency of $CH_3NH_3PbI_3$ Perovskite upon Controlled Exposure to Humidified Air. *J. Am. Chem. Soc.* **2015**, *137*, 1530−1538.
(29) Lee, J. S.; You, K. H.; Park, C. B. Highly Photoactive, Low Bandgap TiO_2 Nanoparticles Wrapped by Graphene. *Adv. Mater.* **2012**, *24*, 1084−1088.
(30) Yan, J.; Ye, Q.; Zhou, F. Polymer Brushes Assisted Loading of High Density CdS/CdSe Quantum Dots onto TiO_2 Nanotubes and the Resulting Photoelectric Performance. *RSC Adv.* **2012**, *2*, 3978−3985.
(31) Chen, H.; Wang, Q.; Lyu, M.; Zang, Z.; Wang, L. Wavelength-switchable Photocurrent in a Hybrid TiO_2-Ag Nanocluster Photoelectrode. *Chem. Commun.* **2015**, *51*, 12072−12075.
(32) Wang, L.; Sasaki, T. Titanium Oxide Nanosheets: Graphene Analogues with Versatile Functionalities. *Chem. Rev.* **2014**, *114*, 9455−9486.
(33) Kapilashrami, M.; Zhang, Y.; Liu, Y.-S.; Hagfeldt, A.; Guo, J. Probing the Optical Property and Electronic Structure of TiO_2 Nanomaterials for Renewable Energy Applications. *Chem. Rev.* **2014**, *114*, 9662−9707.
(34) Banerjee, B.; Amoli, V.; Maurya, A.; Sinha, A. K.; Bhaumik, A. Green Synthesis of Pt-doped TiO_2 Nanocrystals with Exposed (001) Facets and Mesoscopic Void Space for Photo-splitting of Water Under Solar Irradiation. *Nanoscale* **2015**, *7*, 10504−10512.
(35) Tao, J.; Luttrell, T.; Batzill, M. A Two-Dimensional Phase of TiO_2 with a Reduced Bandgap. *Nat. Chem.* **2011**, *3*, 296−300.
(36) Yu, H.; Zhao, Y.; Zhou, C.; Shang, L.; Peng, Y.; Cao, Y.; Wu, L.-Z.; Tung, C.-H.; Zhang, T. Carbon Quantum dots/TiO_2 Composites for Efficient Photocatalytic Hydrogen evolution. *J. Mater. Chem. A* **2014**, *2*, 3344−3351.
(37) Zhang, L.; Li, L.; Cao, Y.; Yao, X.; Ge, C.; Gao, F.; Deng, Y.; Tang, C.; Dong, L. Getting Insight into the Influence of SO_2 on TiO_2/CeO_2 for the Selective Catalytic Reduction of NO by NH_3. *Appl. Catal., B* **2015**, *165*, 589−598.
(38) Hasobe, T.; Imahori, H.; Fukuzumi, S.; Kamat, P. V. Nanostructured Assembly of Porphyrin Clusters for Light Energy Conversion. *J. Mater. Chem.* **2003**, *13*, 2515−2520.
(39) Mok, S. M.; Yan, F.; Chan, H. L. W. Organic Phototransistor Based on poly(3-Hexylthiophene)/TiO_2 Nanoparticle Composite. *Appl. Phys. Lett.* **2008**, *93*, 023310.
(40) Horikoshi, S.; Watanabe, N.; Hidaka, H.; Serpone, N. Photocurrent Enhancement from an Active Hybrid TiO_2 Film Electrode Fabricated by a Sol-Gel Method: Photocurrent Generation during the Photooxidation of 4-Nonylphenol and 4-Nonylphenol Polyethoxylate on TiO_2/OTE Electrodes. *New J. Chem.* **2002**, *26*, 1161−1166.
(41) Chen, S.; Li, Y.; Wang, C. Visible-light-driven Photocatalytic H_2 Evolution from Aqueous Suspensions of Perylene Diimide Dyesensitized Pt/TiO_2 Catalysts. *RSC Adv.* **2015**, *5*, 15880−15885.
(42) Das, J.; Siram, R. B. K.; Cahen, D.; Rybtchinski, B.; Hodes, G. Thiophene-modified Perylenediimide as Hole Transporting Material in Hybrid Lead Bromide Perovskite Solar Cells. *J. Mater. Chem. A* **2015**, *3*, 20305−20312.
(43) De, S.; Dutta, S.; Patra, A. K.; Bhaumik, A.; Saha, B. Self-Assembly of Mesoporous TiO_2 Nanospheres via Aspartic Acid Templating Pathway and Its Catalytic Application for 5-Hydroxymethyl-furfural Synthesis. *J. Mater. Chem.* **2011**, *21*, 17505−17510.
(44) Hartnett, P. E.; Dyar, S. M.; Margulies, E. A.; Shoer, L. E.; Cook, A. W.; Eaton, S. W.; Marks, T. J.; Wasielewski, M. R. Long-lived Charge Carrier Generation in Ordered Films of a Covalent Perylenediimide-diketopyrrolopyrrole-perylenediimide Molecule. *Chem. Sci.* **2015**, *6*, 402−411.
(45) Liu, H.; Shen, L.; Cao, Z.; Li, X. Covalently Linked Perylenetetracarboxylic Diimide Dimers and Trimers with Rigid "J-type" Aggregation Structure. *Phys. Chem. Chem. Phys.* **2014**, *16*, 16399−16406.
(46) Liu, K.; Yao, Y.; Kang, Y.; Liu, Y.; Han, Y.; Wang, Y.; Li, Z.; Zhang, X. A Supramolecular Approach to Fabricate Highly Emissive Smart Materials. *Sci. Rep.* **2013**, *3*, 2372.
(47) Lim, J. M.; Kim, P.; Yoon, M.-C.; Sung, J.; Dehm, V.; Chen, Z.; Würthner, F.; Kim, D. Exciton Delocalization and Dynamics in Helical π-stacks of Self-assembled Perylene Bisimides. *Chem. Sci.* **2013**, *4*, 388−397.
(48) Nanda, J.; Biswas, A.; Banerjee, A. Single Amino Acid Based Thixotropic Hydrogel Formation and pH-dependent Morphological Change of Gel Nanofibers. *Soft Matter* **2013**, *9*, 4198−4208.
(49) Basu, K.; Baral, A.; Basak, S.; Dehsorkhi, A.; Nanda, J.; Bhunia, D.; Ghosh, S.; Castelletto, V.; Hamley, I. W.; Banerjee, A. Peptide Based Hydrogels for Cancer Drug Release: Modulation of Stiffness, Drug Release and Proteolytic Stability of Hydrogels by Incorporating D-amino Acid Residue(s). *Chem. Commun.* **2016**, *52*, 5045−5048.

DOI: 10.1021/acs.jpcc.7b00874
J. Phys. Chem. C 2017, 121, 5428−5435

(50) Roy, S.; Banerjee, A. Amino Acid Based Smart Hydrogel: Formation, Characterization and Fluorescence Properties of Silver Nanoclusters within the Hydrogel Matrix. *Soft Matter* **2011**, *7*, 5300−5308.
(51) Jiao, Y.; Liu, K.; Wang, G.; Wang, Y.; Zhang, X. Supramolecular Free Radicals: Near-infrared Organic Materials with Enhanced Photothermal Conversion. *Chem. Sci.* **2015**, *6*, 3975−3980.
(52) Wei, D. Dye Sensitized Solar Cells. *Int. J. Mol. Sci.* **2010**, *11*, 1103−1113.

DOI: 10.1021/acs.jpcc.7b00874
J. Phys. Chem. C 2017, 121, 5428−5435